About MoO3 as buffer layer in organic optoelectronic devices, Technology Letters

Christian Bernède, Linda Cattin, Mustapha Morsli

ABOUT MoO$_3$ AS BUFFER LAYER IN ORGANIC OPTOELECTRONIC DEVICES

J. C. Bernède[1], L. Cattin[2], M. Morsli[3]

1- L'UNAM, Université de Nantes, MOLTECH-Anjou, CNRS, UMR 6200, 2 rue de la Houssinière, BP 92208, Nantes, F-44000 France.
2- Université de Nantes, Institut des Matériaux Jean Rouxel (IMN), CNRS, 2 rue de la Houssinière, BP 32229, 44322 Nantes cedex 3, France
3- L'UNAM, Université de Nantes, Faculté des Sciences et des Techniques, 2 rue de la Houssinière, BP 92208, Nantes, F-44000 France.

Abstract: MoO$_3$ is well known as efficient anode buffer layer in optoelectronic devices. Actually, MoO$_3$ can be easily deposited under vacuum, by sublimation for instance, and also by wet process. So it is known from a long time that the films deposited by sublimation are amorphous and slightly oxygen deficient, which induces a light blue coloration due to oxygen vacancies. These oxygen vacancies imply the presence of Mo^{4+} and Mo^{5+} in the films. The presence of oxygen vacancies increases the conductivity from 10^{-12} to 10^{-6} (Ωcm)$^{-1}$, while stoichiometric films are insulating and MoO$_2$ has a metallic like behaviour with $\sigma = 2 \cdot 10^2$ (Ωcm)$^{-1}$. About the efficiency of MoO$_3$ as buffer layer, recent studies questioned the MoO3 band structure generally admitted. Under ultra high vacuum, the measured ionisation energy, IE, and electron affinity are found to be 9.7 eV and 6.7 eV respectively, while the films are strongly n-type. Its means that the very large IE energy of the MoO$_3$ excludes any hole transport via the valence band, while the energy alignment between the band conduction minimum, CB, of MoO$_3$ and the Highest Occupied Molecular Orbital (HOMO) of the organic material is favourable for electron transfer between the two materials. In the case of organic photovoltaic cells, the photogenerated hole recombines with an electron at the interface between MoO$_3$ and the organic layer. Indeed, the work function, WF, of the molybdenum oxide films depends strongly of its composition, WF decreases when the oxygen deficiency increases, and on the exposition, or not, of its surface to air contamination. This makes that WF varies from 6.9 eV for a layer studied under ultra high vacuum to 5.2 eV for a layer exposed to the air a few hours. However, since the initial value of WF is very high, MoO$_3$ remains effective if the Highest Occupied Molecular Orbital of the organic material is lower than 6 eV. The band structure of MoO$_3$ and the large possible variations of WF make that, for specific conditions of preparation and conditioning, MoO$_3$ can also be used as CBL.

Keywords: transition metal oxide, organic optoelectronic device, buffer layer, molybdenum trioxide, organic photovoltaic cells.

1. INTRODUCTION

Nowadays, due to its exceptional efficiency as buffer layer in optoelectronic devices, the molybdenum oxide, MoO3, is the subject of a very big interest as shown by the numerous publications which are dedicated to it these last years. It turns out that within the framework of its application as buffer layer, a controversy took birth concerning the band structure of MoO3 and this one is presented in a recent article of synthesis above transition metal oxides for organic electronic [1]. As a matter of fact, the studies devoted to MoO3 did not begin these last years and numerous works were dedicated to it during the second half of the last century. MoO3 belongs to the transparent metal oxides (TMO), which exhibit original properties due to the transition metal. Actually, transition metals have their d orbitals partially filled, which in solids, induces the formation of narrow d bands. The 2p orbitals of TMO, which originate from the oxygen anion, are completely filled. They form the valence band, while the 3d bands, which originate from the metallic cation, are completely empty at 0 K and form the conduction band. In the case of molybdenum oxides, if stoichiometric MoO3 is insulating, MoO2 has a metallic conductivity, while sub-stiochiometric MoOx have semi-conducting properties. Usually, MoO3 crystallizes in the α-MoO3 orthorhombic structure, but others structures are possible.

In the present work, we focus our interest on MoO3 thin films, being interested by its application to organic optoelectronic devices. In the section 2, we recall that very interesting works were dedicated to MoO3 thin films well before that people are interested in its application in organic optoelectronic devices. In section 3, its use as anode buffer layer is described. The section 4 is dedicated to UPS-IEPS experimental studies, studies which question the MoO3 bands structure generally accepted before. Then in section 5, according to the debate opened by these measures giving new values for the MoO3 band structure, we discuss the different models proposed to justify the efficiency of MoO3 as anode buffer layer. A new controversy is now opened about its effect on device performances, when MoO3 is used as cathode buffer layer, it is discussed in the last part of section 5. Our discussion leans on a study led in the laboratory. Some perspectives are given as conclusion.

2. MoO$_3$ THIN FILMS GENERALITIES

It is remarkable that many old publications present very interesting studies which often describe results which are nowadays presented as new. The article of Deb and Chopoorian, which dates of about half a century, presents a very complete optical study of MoO3 thin films deposited by sublimation [2]. The films, thick of 100-245 nm, are deposited at very high speed (17±1.5 nm/s). The composition of the films is identical to that of the starting material. After sublimation, the films are amorphous, with an optical band gap, Eg, of 3.1 eV and a refractive index n = 2.38. The formation of colour centres is also studied, it will be discussed below. MoO3 films were also deposited by rf-sputtering [3]. Here, a MoO3 compressed powder is sputtered by an Ar-O2 gas mixture onto a substrate heated at 200°C. The properties of the films depend on the oxygen relative concentration. For instance, the electrical resistivity of the films increases with increasing oxygen concentration from 2.5x1010 to 1x1012 Ωcm. The refractive index n = 2.01 to 2.26, while the band gap varies from 2.67 to 2.76 eV. Reactive sputtering was also used as deposition technique of MoO3 [4, 5]. Starting from Mo targets, depending on the oxygen partial pressure during sputtering, the films crystallize in either the thermodynamically stable orthorhombic α-MoO3 or a new metastable monoclinic β-MoO3 phase, while the films deposited on cooled substrates are amorphous [4]. Here again n and Eg were measured, n = 2.3, while Eg = 3.1. It is possible, by varying the power supplied to the magnetron source, to deposit films with composition continuously ranging from MoO3 to Mo2O. This observation of many non-stoichiometric compounds suggests interstitial occupancies within a host lattice framework [5].

Another MoO3 deposition technique used since a long time is the chemical vapour deposition (CVD) [6-8]. CVD allows achieving MoO3 thin films when molybdenum hexacarbonyl Mo(CO)6 is used as precursor. More precisely, after deposition of black molybdenum, MoO3 is achieved by annealing in air these black molybdenum films. At 500°C to 600°C, these films become transparent, they crystallize in the orthorhombic modification of MoOx. Depending on the annealing conditions the band gap varies from 2.70 to 3.1 eV and n from 2.15 to 3.2.

MoO3 films can be achieved using MoS2 as precursor, either starting from suspension of monomolecular layers of MoS2 in water [9] or by substitution of the chalcogen of pre-textured chalcogenide film [10]. Such technique allows achieving textured films. In both cases MoO3 thin films crystallized in the orthorhombic structure are obtained with their crystallites oriented along the (0k0) direction. The resistivity of these films is ρ= 2x106 ohm.cm.

Table.1. Raman peaks of MoO3 and MoO2 [11].

| Material	Raman peaks (cm^{-1})							
MoO$_3$	997	821	668	379	338	293	285	244
MoO$_2$	744	589	571	495	461	363	228	203

In a more than 20 years old manuscript [11] an exhaustive and actual study by X-ray photoelectron spectroscopy (XPS) and Raman spectroscopy of the progressive thermal reduction of MoO3 film is proposed. The MoO3 films are grown directly onto Mo substrate by heating in air at 250°C for 4h. Then, they are progressively reduced in hydrogen or nitrogen gases at a temperature range 350-730°C. The binding energies measured for the different Mo oxidation states (Mo° to Mo6+) are given in table 1. The measured values are in good agreement with far more recent studies. The Raman spectroscopy study shows that it is a powerful technique to discriminate between the two phases of molybdenum oxides: MoO$_3$ and MoO$_2$ (Table 2).

Table.2. Binding energy of Mo3d$_{5/2}$ for the different oxidation states of Mo [11].

| Oxidation state	Mo°	MoO$_3$	MoO$_2$	Mo^{4+}	Mo^{5+}	Mo^{6+}
Binding energy (eV)	227.7	232.7	229.2	230.1	231.2	232.6

As evocated above, just like WO$_3$, MoO$_3$ is known for its electrochomic and photochromic properties [2, 12, 13]. On irradiating MoO$_3$ thin films with light of wavelength shorter than 330 nm, three absorption bands due to color-centers are formed. The same type of color-centers is formed by heating in inert atmosphere. These color-centers cannot be bleached optically. However they can be bleached thermally in

oxygen atmosphere at 300°C. The formation of the color-centers is associated with increased dark conductivity of the MoO3. The study is completed by ESR experiments. It is shown that the ESR signal, g = 1.924, which is due to the presence of Mo5+, disappears after heating, ie after bleaching of the color-centers. It is concluded that the color centers are formed as a result of free electrons being trapped in oxygen ion vacancies [2]:

$$MoO_3 - \frac{1}{2} x \, O_2 = [Mo_{1-2} x^{6+} Mo_2 x^{5+}] O_{3-} x \, \square \, x$$
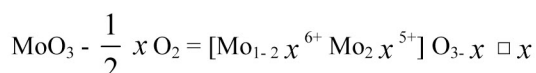
Electrochomism and photochromism were also encountered in films deposited by electron beam evaporation [12]. In the presence of steam there is possibility of film colouring, not under vacuum. It corresponds to a Red-Ox reaction:

H+ reduction:

$$MoO_3 + xH + +xe- \longrightarrow Mo_{3-x}(OH)_x$$
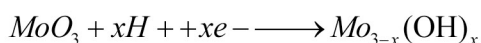
In the same way, amorphous films of MoO_3, deposited by thermal evaporation, can be coloured using NH_2SO_4 as
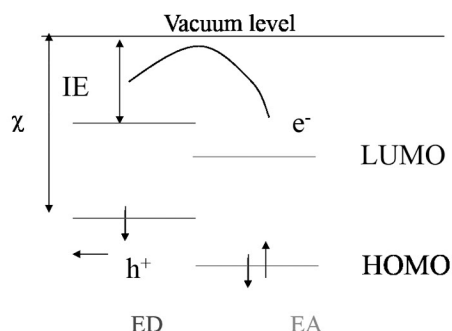

Figure 1: Scheme of the band structure at the contact electron donor/electron acceptor.

electrolyte [13]. A strong absorption band appears, at around 900 nm, in the optical spectrum of coloured films. Another example is given by the MoO_3 films deposited by rf sputtering [3]. These films exhibit the required properties for their use in electrochromic display, in presence of $LiClO_4$, under a dc polarization of 0.5 V, MoO_3 is coloured by the Li+ ions.

Some general information can be extracted from these previous studies:
- *MoO_3 thin films can be easily deposited by simple Joule effect sublimation,*
- *These films are amorphous and slightly oxygen deficient, which induces a light blue coloration due to oxygen vacancies.*
- *These oxygen vacancies imply the presence of Mo^{4+} and Mo^{5+} in the films.*

- *These films are electrochromic.*
- *Stoichiometric films are insulating,*
- *The presence of oxygen vacancies increases the conductivity from 10^{-12} to 10^{-6} $(\Omega cm)^{-1}$,*
- *MoO_2 has a metallic like behaviour with $\sigma = 2 \, 10^2$ $(\Omega cm)^{-1}$ [8].*
We must keep in mind these informations while we are going to be interested in the current applications of MoO_3.

3. MoO3 as anode buffer layers in organic optoelectronic devices

As evocated previously, organic optoelectronic devices such as organic photovoltaic cells (OPVs) and organic light emitting diodes (OLEDs) are nowadays the subject of a very large numbers of studies because of their lightness, flexibility, easiness to achieve… Roughly, such devices are constituted by an active organic film sandwiched between two electrodes, one of them being transparent and the other one being highly reflexive. More precisely, the active organic film corresponds to two constituents, one of them is called the electron donor (ED) and the other is called the electron acceptor (EA). The electric field present at the contact ED/EA permits the charge separation of the carriers bounded in the exciton formed after light absorption by one of the organic material, usually the ED. As a matter of fact, the ED and EA must have their relative electron affinity, (Lowest Unoccupied Molecular Orbital-LUMO) and ionisation energy, (Highest Occupied Molecular Orbital-HOMO) well adapted. The electron affinity of the donor is smaller than that of the acceptor, while the ionisation energy (IE) of the acceptor should be significantly greater than that of the donor. The electric field results from this band structure configuration (Figure 1). Based on these foundations, two OPV families are under investigation. The first one is based on a blend of the ED and EA, the ED being usually a polymer and the EA a fullerene derivative (Figure 2). The second is based on planar heterojunction (Figure 3). Each of them has their advantages and disadvantages.

For effective light absorption, the organic semiconductor film thickness should be at least 100 nm, since the typical diffusion length of the exciton is 10-20 nm and since the exciton dissociation is effective at donor/acceptor interface, one possibility is to use a blend of the donor and the acceptor, as said above, this concept is called "bulk heterojunction (BHJ) [14]. The BHJ allows improving power efficiency by increasing the area of interface between the electron donor and the electron acceptor, through spontaneous phase segregation of both phases. The first difficulty encountered in such dispersed heterojunction is that of solid state miscibility and stability. Usually organic conjugated systems are not miscible. Therefore the blend should be fabricated out of

equilibrium. Spin coating, ink jet printing and also co-evaporation can be used. However the morphology of these BHJ is difficult to control. The spontaneous phase separation results in a disordered morphology, with cul-de-sac regions that impede transport of charge to the electrodes (Figure 2) [15].
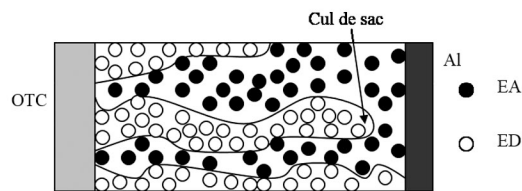

Figure 2: Schematized bulk heterojunction.

Recent improvement of the performance of small molecules OPV cells induces a new growing interest for the planar heterojunctions [16]. These OPV cell are based on an organic bilayer, sandwiched between two electrodes. The bilayer is an heterojunction, between an ED and an EA. The advantages of these structures are: easy control of the structure (thickness, morphology, number of films…) high flexibility in the cells growth, purity, reproducibility.
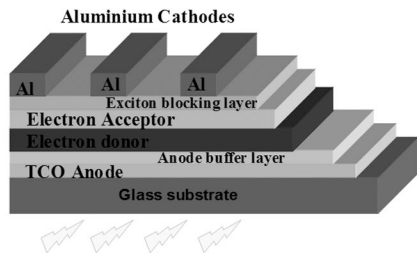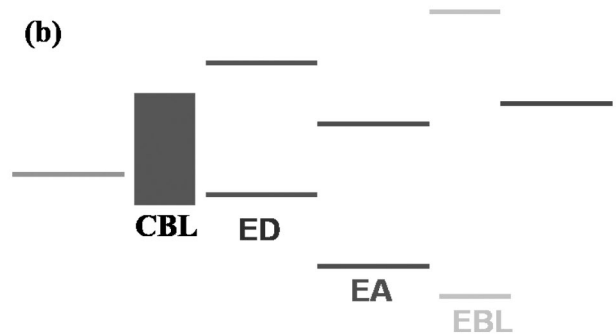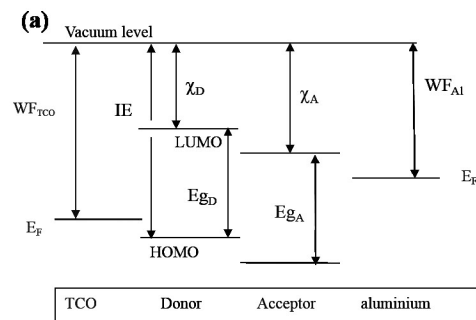

Figure 3: Schematized planar heterojunction.

Figure 4: Schematic representation of the band scheme of OPV without (a) and with (b) buffer layer.

About the electrodes, while aluminium, or silver, is often used as reflexive cathode, it is well known that the transparent conductive anode which gives the best optoelectronic devices is the indium tin oxide (ITO). It is admitted, in order to achieve high efficiency, that the use of performing organic materials is necessary but not sufficient because after the absorption of the light and the charge separation it is necessary to collect the carriers, which means that nearly ohmic contact with the electrodes are necessary. For instance, often, the hole exchange at the interface ED/anode is a limiting factor of the device performance.
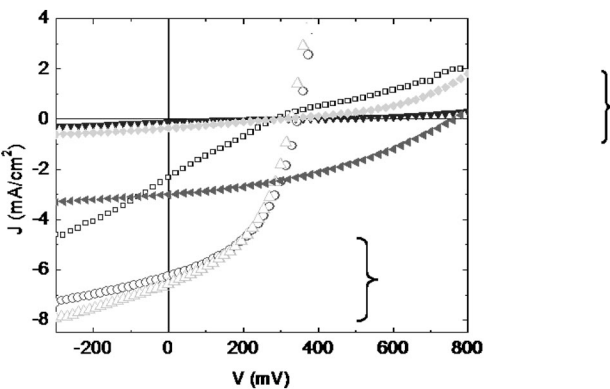

Figure 5: J-V characteristics of OPV cells using Au ABL(open symbols) and MoO3 ABL (full symbols) for EDs with different HOMO values.

To circumvent this difficulty buffer layers are often introduced between the electrodes and the organic materials (see for instance Figure 3). The buffer layer between the anode and the ED is the anode buffer layer (ABL) and that between the cathode and the EA is the cathode buffer layer (CBL) which is, as we will see below, often called exciton blocking layer (EBL), at least in the case of planar heterojunctions. In the classical configuration, the cathode is the top electrode and it must be highly reflexive for improving light absorption, mainly in the case of planar heterojunctions. Also its work

8

function must be as low as possible. Therefore the metal used is either Al or Ag.

The transparent electrode, which allows the photons to interact with the organic absorbing layer, is usually an ITO film deposited onto the glass substrate.

Schematized band scheme representations of planar OPV without and with buffer layer are presented in figure 4, it can be seen that without buffer layers, potential barriers are present at the interfaces electrode/organic material.

As said above, efficient charge collections are usually achieved through electrode buffer layers. As a matter of fact, for efficient charge collection, work functions of cathode and anode must be matched to the lowest unoccupied molecular orbital (LUMO) of acceptor and the highest occupied molecular orbital (HOMO) of donor, respectively. Buffer layers (BF) are necessary in view of the difficulties in organic optoelectronic devices of the charge carrier transport between the organic materials and the electrodes. More specifically, in the case of CBL, in planar heterojunction, the CBL avoid the quenching of the exciton by the metal. Such CBL was called exciton blocking layer (EBL) [17]. It has been proposed also that it can prevent damage to the electron acceptor film during cathode deposition, and behaves as optical spacer. If the EBL block the excitons, it should not block all charge carriers. However the offset energy of the HOMO of the electron donor (often the fullerene) and the EBL (such as the bathocuproine) is large. Moreover, the optimum EBL thickness is 8-9 nm, which is too tick to allow high tunnelling current. So it has been suggested that the charge transport in the EBL is due to aluminium diffusion during deposition of the cathode [17].

In the case of the anode/electron donor contact, a common solution is to introduce a thin ABL, which adjusts the electronic behaviour of the adjacent materials. For instance, when CuPc is the ED, we have shown that an ultra-thin (0.5 nm) Au film introduced between the anode and the organic material can be used to improve the devices performances [18, 19].

As a matter of fact, if the work function, WF, of ITO is only 4.8 eV, the HOMO of CuPc is 5.2 eV and WF of Au is 5.1 eV. Therefore, the Au improves significantly the band matching between CuPc and the anode. The importance of the band matching on the OPV cells performance is consolidated by the study which we led on the effect of the HOMO value of the ED on the performances of the OPV cells. If Au is a very efficient ABL when the HOMO is around 5 eV, when it is around 5.5 eV, which is the case when the ED is tetraphenyldibenzoperiflanthene (WF_{DBP} = 5.4 eV), thienylenevinylenetriphenylamine functionalized with per heral dicyanovinylene groups ($WF_{TDCV-TPA}$ = 5.8 eV), it does not work anymore (Figure 5).

On the contrary, MoO_3 is efficient whatever the HOMO value is (Figure 5) [20, 21]. As a matter of fact, it was shown before that MoO_3 is an efficient hole injecting layer in OLEDs [22, 23] and, in the same way, a promising ABL in OPV cells [24, 25]. Usually, in the first works describing the interest in using MoO_3 buffer layers, it is supposed that it is a p-type semiconductor with the summit of its valence band (VB) situated at 5.3 eV below the vacuum level, which could induce a better band matching at the interface anode/ED and justifies the positive effect of MoO_3. However, contrarily to Au, MoO_3 is efficient with ED exhibiting an HOMO value significantly higher than 5.3 eV. Moreover we showed that whatever the depositing process of MoO_3, sublimation [26] or electrochemical process [27], it works as ABL, even if the surface properties of both kinds of films must be quite different. More precisely it could be noted that, in the case of electrochemistry, the MoO_3 films are efficient only when Mo^{5+} are present in the films. All this made that if the effect of Au on the OPV cells performances appears easy to understand (Figure 6) that of MoO_3, which is more universal, is not so simply understandable.

4. Ultra-violet photoemission spectroscopy and inverse photoemission spectroscopy of MoO_3 thin films.

For the investigation of the chemistry and electronic properties of interfaces, X-ray photoelectron spectroscopy (XPS) and ultraviolet photoelectron spectroscopy (UPS) and inverse photoemission spectroscopy (IPES) are valuable tools. Before presenting the MoO_3 study by these techniques, we shortly recall the bases of these techniques and some generalities on the behaviour of metal/organic semiconductors interfaces [28]. Usually, the direct and inverse spectroscopies (UPS and IPES) are realized in situ under ultra high vacuum. UPS was done with helium discharge lamps using two specific radiation lines, HeI ($h\upsilon$ = 21.22 eV) and HeII ($h\upsilon$ = 40.8 eV). IPES was done using a low energy electron gun and a detector of photons.
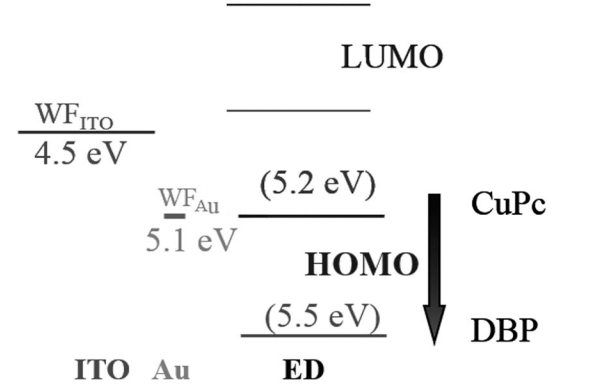

Figure 6: Schematized band scheme of the contact ITO/ABL/ED with ED with different HOMO values.
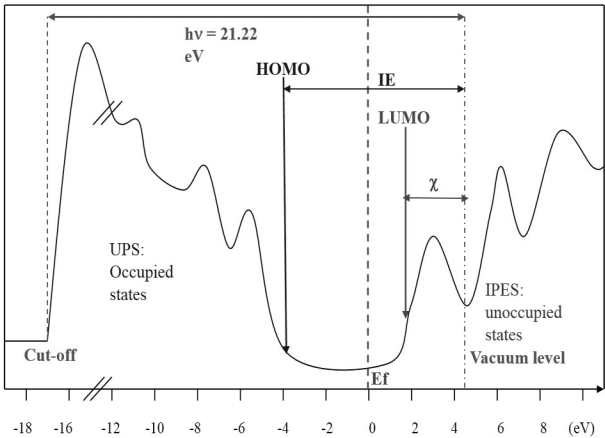
Figure 7: Schematized presentation of combined UPS and IPES spectra.

The electron of weak energy penetrates into the solid above the vacuum level and decay in an empty state. The energy so released gives a photon, which is captured by the detector. The number of photons collected according to the energy of the electron gives the density of unoccupied states in the studied solid (Figure 7). The UPS spectrum gives the HOMO with regard to the Fermi level Ef, while the IPES spectrum gives the LUMO. The difference between them is the band gap of the material Et, not to confuse with the optical band gap Eg, which gives the energy necessary for the formation of an exciton. Then Et-Eg corresponds to the binding energy of the exciton. At the left part of the UPS spectrum the secondary electron cut-off provides a direct measure of the vacuum level of the sample. Actually, the source of energy hυ can extract electrons, i.e. carry them to the vacuum level, only after having overcome their binding energy in the atom and the energy to carry them from the surface of the atom to the vacuum level. Thus the cut-off allows measuring WF:

$$WF = (h\nu - cut\text{-}off)_{Ef=0}$$

In figure 8, we present the electronic structure of typical metal/organic semiconductor interface. The density of interface gap states, D, is schematically represented at the interface between the HOMO and LUMO, while the shift between the vacuum level of the two materials is called χ. As a matter of fact, after deposition of an organic monolayer, possible shifts of the cut-off and thus of the vacuum level suggest the formation of an interfacial dipole layer Δ [29, 30] (Figure 8). In this case the small binding energy onset corresponds to the emission from the highest occupied molecular orbital (HOMO) and the high binding energy (low kinetic energy) cut-off corresponds to the vacuum level at the surface of the organic layer. Therefore as said above we can visualise

the relative position of the energy levels at the interface, and examine the difference of the vacuum level between the metal and organic layer which corresponds to Δ (Figure 8).
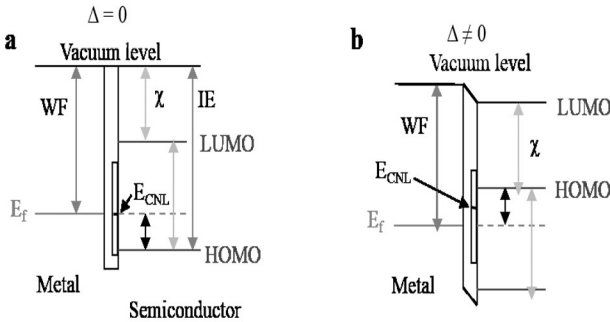

Figure 8: Interfacial dipole Δ after contact: a: Δ = 0,   b : Δ ≠ 0.

In figure 8 E_{CNL} is the charge neutrality level of the interface states. If Ef is below (above) E_{CNL} the net charge in the interface states is positive (negative) and a positive (negative) dipole develops across the interface. The occurrence of a dipole is due to the presence of interface states. The main contribution is the induced interface states, which are due to the overlap between continuum of metal states and organic semiconductor molecular levels, which broaden the latter and induces a density of interface states in the gap of the organic semiconductor [31].

The total charge of the density of interface states is null if the Fermi level, Ef, aligns with E_{CNL} and it is negative or positive if it is above or below it. Therefore the metal work function of the electrode is very important in determining the barrier height at the interface. However, the range of work function of metal and transparent conductive oxides which can be used as electrode is relatively limited. So, electrode surface modification is necessary and, as said above, MoO_3 is one of the most successful anode buffer layer, which justify its characterisation by UPS and IPES spectroscopies.

Recent studies, using UPS and IPES measures, questioned the MoO_3 band structure usually accepted, namely the p-type and the value of WF. Actually, UPS and IPES are highly performing techniques which allow measuring with precision the band structure. In a reference work Kröger et al show that the values of IE, χ and WF are very superior to those admitted before [32]. In this study, MoO_3 is deposited onto ITO in ultra high vacuum (around 10^{-7} Pa). The UPS study shows that WF = 6.86 eV and WF-VB = 2.82 eV, which means that IE = 9.68 eV. The IPES study gives χ= 6.7 eV, i.e. 0.16 eV above WF, which means that MoO_3 is deeply n-type. The n-type is related to the existence of oxygen vacancies,
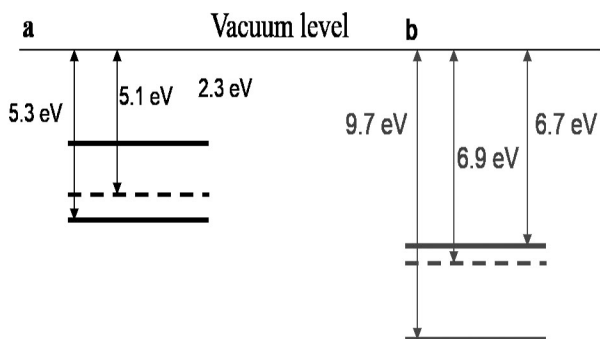
Figure 9: Old (a) and new (b) scheme of the MoO3 band structure.

which increase the film conductivity, even if only Mo^{6+} are detected by XPS. The new measured values are presented in figure 9 where they can be compared with the old usually accepted values.

It is interesting to note that, while the p-type of MoO_3 was admitted by the scientific community, in a pioneer work, Sian and Reddy showed that sublimated MoO_3 thin films were n-type, with Mo^{4+} and Mo5+ present in the films due to oxygen deficiency in as-deposited films [figure 9 ref. 33].

In the same spirit than in ref 32, Greiner et al [34] proceeded to a systematic study of the different oxidation states of Mo. They start from the molybdenum metal, which $Mo3d_{5/2}$ is 228 eV. Then they oxidize the Mo to achieve MoO_3, here the oxidation state of Mo is Mo^{6+} and $Mo3d_{5/2} = 232.4$ eV. Then they reduce the oxide to $Mo0_{2.5}$ by annealing under vacuum. The reduced oxide contains Mo^{4+} and Mo^{5+} with a metallic band structure similar to MoO_2, here the binding energy of $Mo3d_{5/2}$ is 229.3 and 231.2 eV for Mo^{4+} et Mo $^{5+}$ respectively. The UPS study allows measuring the work function of Mo in its different oxidation states: 6.8, 5.9, 4.7 eV for MoO_3, MoO_x and Mo respectively. Here also the oxide films are n type. In the case of fully oxidized Mo, the WF value is nearly equal to that measured by Kröger et al (figure 9). Moreover, it can be concluded that the value of WF varies with the oxidation state of the oxide. Irfan et al [35] show that air exposition of MoO_3 thin films induces a significant decrease of its WF. The WF surface value gradually changes from 6.8 to 5.3 eV for air exposed films, while for oxygen exposed films, WF saturated at 5.7 eV. It corresponds to two distinct stages of exposure, one dominated by oxygen absorption and the other by moisture absorption. This surface WF evolution is corroborated by a study of the Kröger group which shows that, while after deposition under ultra high vacuum, WF = 6.8 eV, after 1-3 min of room air exposure, WF decreases of 1 eV and CB = 5.5 eV while VB = 8.6 eV,

CB being the bottom of the conduction band. They also show that the value of the dipole created at the interface MoO_3/organic material depends on the history of the MoO_3 layer and on the HOMO value of the organic material. In the case of N,N′-bis(1-naphthyl)-N,N′-diphenyl-1,1′-biphenyl-4,4′-diamine (α-NPD), which HOMO is 5.4 eV, the decrease of WF after air exposure is compensated by the decrease of the dipole value, at the interface after contact, which means that, finally, the band matching at this interface does not depends of the air exposure. Actually, while WF decreases from 6.7 to 5.5 eV when submitted to air, simultaneously decreases from 2.1 eV to 0.9 eV [36].

Nevertheless, in another study [35], it is shown that, after air exposure, following the decrease of its WF, the efficiency of MoO_3 as buffer layer is limited to ED which WF < 5.9. For higher HOMO value, some limitation of the current of the device is possible [1, 37]. This last result is corroborated by another study dedicated to the effect of air exposure on the efficiency of MoO_3 as ABL [38]. Here WF decreases from 6.8 eV before air exposure to 5.16 eV after air exposure of one hour. However the study shows that when the HOMO of the organic material is smaller than 6 eV, the hole injection barrier remains unchanged after air exposure, while for organic material with HOMO value higher than 6 eV there is s significant increase of the hole injection barrier. As known, the films deposited by sublimation under vacuum are deficient in oxygen and Mo^{5+} and Mo^{4+} are detected by XPS. Surprisingly, after air exposition, the reduced species are not oxidized as expected. Instead the authors measure by XPS a significant increase of these reduced species, which suggest that the air exposure induces reduction and not oxidation of the MoO_3 films. They propose that during air exposure, some gas species such as water molecules can undergo oxidative adsorption on MoO_3 films, involving electron transfer from the adsorbates to the underlying MoO_3 films, thereby reducing the MoO_3 and decreasing its surface work function [38].

Using the semidirect XPS method we have estimated the band discontinuities at the interface ITO/MoO_3 ($\Delta Ev = 0.50$ eV, $\Delta Ec = 0.90$ eV) and with a Kelvin probe we have measured the ITO work function (4.7 eV). From these measures we can estimate to 8.4 and 5.8 eV the IE and χ values of MoO_3. These measures are in compliance with the values measured by the other groups after air contamination [36-38].

Therefore, it can be concluded from the UPS-IPES study that if the MoO_3 thin films are systematically and strongly n-type, which is due to oxygen vacancies, while its WF depends strongly of its composition, WF decreases when the oxygen deficiency increases, and on the exposition, or not, of its surface to air contamination.
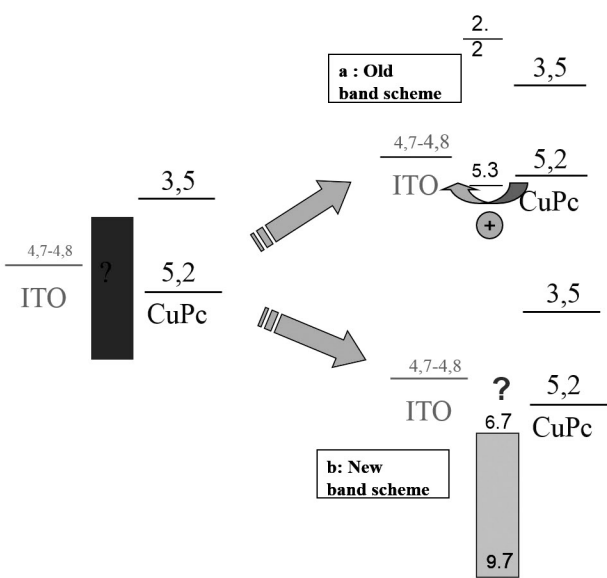
Figure 10: Band scheme of the interface ITO/MoO3/CuPc (a) old band scheme, (b) new band scheme.

5. How does it work?

If we suppose that, as still a lot of searchers [39-41], that the band scheme of figure 9a is the good one, i.e. that IE = 5.3 eV, χ = 2.3 eV, while WF is around 5.1 eV, it can be think that MoO$_3$ allows achieving a good band matching between the anode and the organic material (Figure 10 a). With such band scheme the collection (injection) of hole from (toward) the organic material toward (from) the ITO electrode is facilitated.
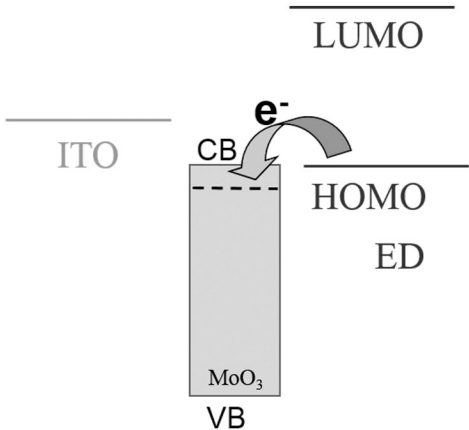

Figure 11: Interface ITO/MoO3/ED, about the collection (injection) of holes.

However, even if there are still many searcher using these values, the UPS-IPES measures proceeded by different groups suggest that the true band scheme is more probably that of figure 10 b [1, 32, 35, 42-46]. With IE =

9.7 eV, the hole transport through valence band is very unlikely, more probably, the MoO$_3$ being strongly n-type, the electron transport via the conduction band is more probable, while, MoO$_3$ being a p-dopant of the organic material it can reduce the barrier height at the interface. Kröger et al propose that [1, 32] (figure 11), the very large IE energy of the MoO$_3$ prohibits any hole transport via the valence band, while the energy alignment between the band conduction minimum, CB, of MoO$_3$ and the HOMO of the organic material is favourable for electron transfer between the two materials. In the case of OPV cells, the photogenerated hole recombines with an electron at the interface between MoO$_3$ and the organic layer, which means that MoO$_3$ works as a charge recombination layer. For OLEDs, under a positive bias applied to the anode, hole injection into the organic film proceeds via an electron transfer from the HOMO of the organic to the band conduction of the MoO$_3$ (figure 11). From this discussion, MoO$_3$ cannot be an electron blocker because its CB edge is too low.

In addition to charge transport via the CB of the oxide, charge transport via gap states in MoO$_3$ can be active. As a matter of fact, gap states due to oxygen deficiency were put in evidence in MoO$_x$. However, the density of gap states, which are clearly due to oxygen deficiency, depends drastically on the formation conditions of the interface. For instance, the stoichiometry of the MoO$_3$ films depends on the deposition conditions. The MoO$_3$ tends towards stoichiometry when the deposition rate increases [47]. Therefore even if the interface behaviour can be explained by the process described above [1], a contribution of transport via gap states cannot be excluded. Different authors use these gap states to justify the behaviour of MoO$_3$ as ABL.
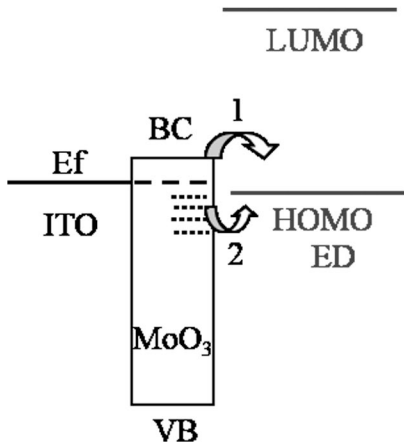

Figure 12: Hole injection from ITO to organic, after surface defect creation, there are two possible routes:(1) injection of electrons into the ED via MoO3 conduction band.(2) injection of electrons from the filled defect states of MoO3.

As a matter of fact, following their study, defects of MoO_3 play a crucial role because in perfectly stoichiometric MoO_3 is insulating. After MoO_3 film deposition and oxidation, defects are generated by surface sputtering and high vacuum annealing. The XPS study shows that Mo^{4+} and Mo^{5+} are present with the Mo^{6+} after defect creation. The defect creation allows an improvement of the short circuit current and of the power conversion efficiency of 50%. The enhancement of the current densities results from an improved hole injection property (from ITO to organic). After surface defect creation, there are two possible routes as shown in figure 12. The first (1) is the injection of electrons into the ED via MoO_3 conduction band. The second pathway (2) of charge transfer is the injection of electrons from the filled defect states of MoO_3. For as-prepared MoO_3, the second route is greatly reduced since the concentration of defects is low. After defect generation the second pathways become significant and the current increases [48].

Another example on the importance of the density of gap states on the devices performances is given by Wang et al [49]. They show that the injected current in organic light emitting diodes is enhanced after a surface sputtering treatment of 5 to 10 s of the MoO_3 layer used as hole injection layer. As a matter of fact the injection current of devices incorporating treated MoO_3 is enhanced by one order of magnitude as compared to that of devices without sputter treatment. The luminance of the diodes is also improved. It is due to the fact that with this slight sputter treatment MoO_3 layers represent lower oxidation states and show metallic characteristics in energy band structure, which remarkably elevates the carrier injection efficiency from ITO to NPB. The work function of the evaporated MoO_3 is 6.2 eV. Since that of pure stoichiometric MoO_3 is 6.8 eV [1] and that of MoO_2 is 5.7 to 5.9 eV, the measured value suggests a mixture of MoO_3 and MoO_2 in the as deposited films, which is reasonable since oxygen deficiency occurs during thermal deposition of MoO_3 layers. After sputtering there is a decrease of the work function indicating that the surface of the MoO_3 layer was altered toward more MoO_2 in composition. Also the band structure is modified with the growth of gap states at 1.1 and then 2.2 eV below the Fermi level. These gap states originate from the partially filled Mo4d bands due to the removal of oxygen atoms. These gap states even connect the original valence band edge of MoO_3 to the position of the Fermi level, giving metallic characteristics. These gap states serve as carrier ladders and provide accessible states for hole to transfer from ITO to the organic layer.

The importance of the gap states on the efficiency of optoelectronic devices is corroborated by studies dedicated to MoO_3 deposited by wet techniques. For instance, after depositing, by spin coating, MoO_x from different solutions Sun et al [50] show that the efficiency

of their inverted OPV cells is increased after air plasma treatment. As a matter of fact they show that after air plasma treatment the Mo/O atomic ratio decreases from 3.03 to 2.71. This MoO_3 reduction allows achieving efficiency of the same order of magnitude than that obtained with MoO_3 deposited by sublimation under vacuum. They attribute this efficiency improvement to the fact that the deficiency of oxygen in the MoO_3 layer would lead to extra states in the forbidden gap of MoO_3, providing another path for hole transport, thus improving the transport and therefore the OPV cell efficiency.

About the interest of this second path for carrier transport, Vasilopoulou et al shown that it not only improve the efficiency of MoO_3 as buffer layer but also that the bang gap states allows using MoO_3 as cathode buffer layer. As a matter of fact, recently, Vasilopoulou et al, have shown that MoO_x films can be used as anode and cathode buffer layer [51, 52]. They deposit their oxide by using a hot-wire vapour assisted technique. When the films are deposited under oxygen partial pressure, stoichiometric MoO_3 films are obtained, while substoichiometric films are obtained when they are deposited in partial hydrogen pressure. Through an XPS study they show that, while only Mo^{6+} are present in the stoichiometric MoO_3 films, Mo^{6+} and Mo^{5+} are present in substoichiometric films. The corresponding work functions are 6.2 eV for the MoO_3 films and 5.9 eV for the MoO_x films.

Moreover, in contrast to stoichiometric MoO_3, the valence spectrum of reduced MoO_x shows a large density of occupied sub-bandgap states centred at 2.2 and 1.1 eV below the Fermi level that are attributed to filled with electrons O2p and Mo4d states respectively. In particular the peak attributed to Mo4d orbital extends up to the Fermi level at almost 0 eV, implying that it has nearly zero band gap and thus it behaves as a degenerated oxide. A study of hole only devices shows that those with MoO_x layer have current two order of magnitude higher than those using MoO_3 using buffer layer. As a matter of fact if MoO_3 allows obtaining a good band matching, it is insulating while MoO_x is not. Interestingly, it is shown that, while the thickness (5-10 nm) of the MoO_x film does not change the current value, that of MoO_3 changes it, due to its poor conductivity [52]. The same group proposes a very original utilisation of MoO_x as cathode buffer layer [51]. They show that the electron injection in an OLED based on Poly[(9,9-di-*n*-octylfluorenyl-2,7-diyl)-*alt*-(benzo[2,1,3] thiadiazol-4,8-diyl)] (F8BT) can be significantly improved by inserting a thin layer (5 nm) of partially reduced molybdenum oxide ($MoO_{2.7}$) between the aluminium cathode and the organic emitting layer.

They attribute this improvement to the occupation with electron of the gap states attributed to Mo4d orbitals. Actually after measuring the valence band maximum energy of MoO_x by UPS to be equal to 7.1 eV, the band gap of MoO_3 being 3 eV, they conclude that the conduction band minimum is at around 4.1 eV, which is in good agreement with the work function of Al (4.3 eV). This energy alignment results in a relatively low electron injection barrier height. In addition the states present in the band gap of MoOx may increase the electron injection from Al and increases the conductivity of the oxide layer.

In the same order of idea, more recently, it was shown that OPV cells efficiency can be improve through the use of a bathophenanthroline/ molybdenum oxide (Bphen/MoO_x) as compound cathode buffer layer [53]. OPV cells based on planar CuPc/C_{60} diodes were used in this work. It is shown that the optimum performance is achieved when the cathode buffer layer is Bphen/MoO_x with thicknesses 2nm/5nm respectively. They attribute this improving effect to the fact that the presence of Bphen prevents the formation of a diode at the contact MoO_3/C_{60}, while the MoO_3 prevents Bphen damaging during Al deposition. In order to justify the good band matching between Al (WF = 4.3 eV), MoO_3 (WF = 5.1-6.2 eV, depending on the experimental conditions) and C_{60} (LUMO 3.7 eV) they propose a dipole value of 3 eV at the interface MoOx/Bphen, value issued from the bibliography. About the protection of Bphen by MoO_3, from Al deposition it should be noted that usually, among the justification of the EBL (bathocuproine, tris-(8-hydroxyquinoline) aluminium (Alq_3) or Bphen) it is often proposed that it protects C_{60} from Al deposition and that the diffusion of Al into the EBL allows electron transfer through this layer. Therefore it seems that the protection of the EBL by the MoO_3 is not clear. Moreover, the WF value of MoO_3 being strongly dependent of its history (deposition and storage conditions), the values stemming from the bibliography must be used with precaution.
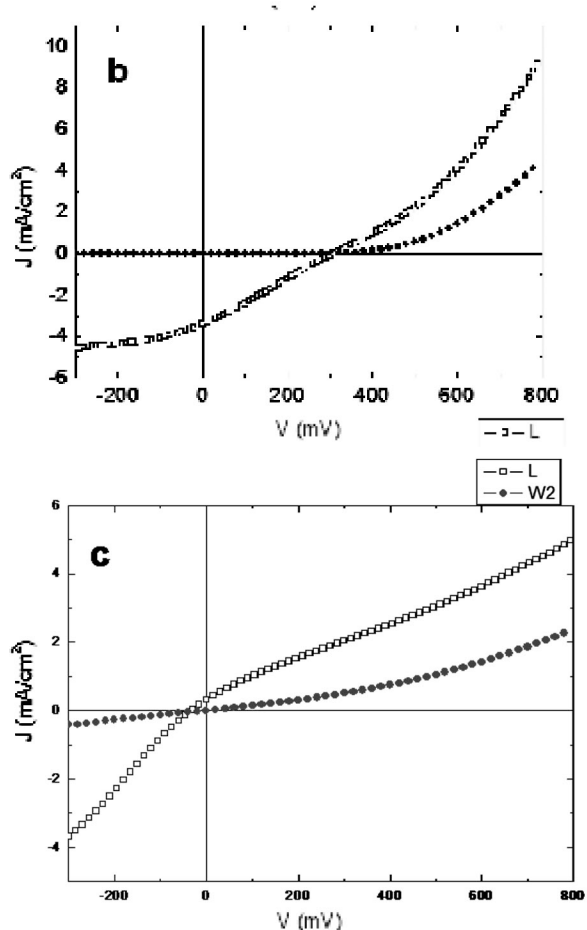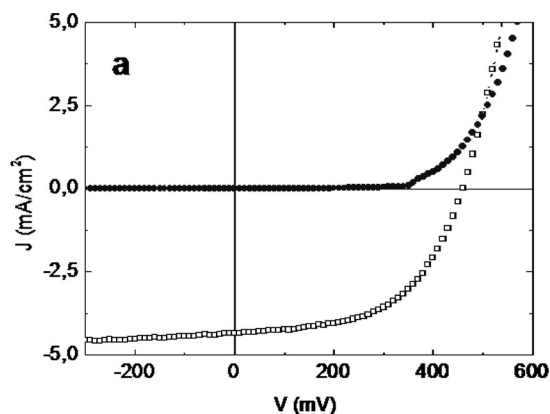

Figure 13: J-V characteristics of OPV cells using (a) Alq3 (9 nm), (b) Alq3 (6 nm) / MoO3 (3 nm) and Alq3 (3 nm)/MoO3 (6 nm) as CBL; in the dark (full symbols) and under light AM1.5 (open symbols).

Indeed, we have probed nearly similar structures in our laboratory and we have obtained very different results. Our OPV cells were ITO/MoO_3/CuPc/C60/Alq_3/MoO_3/Al with different thickness for the constituents of the couple Alq_3/MoO_3. It can be seen that the presence of MoO_3 in the CBL induces systematically a degradation of the OPV cells performances, degradation which gets worse with the increase of the thickness of the MoO_3 layer (Figure 13). When MoO_3 is thick of 2 nm (Figure 13b), the J-V characteristics are S-shaped which is typical of the formation of a reverse diode at a contact electrode/organic material [54, 55]. This effect increases dramatically when the MoO_3 thickness is 4 nm (Figure 13c). This discrepancy must be discussed by using all the results reported above.

The basic ideas which we can deduct of these results are the following ones:

-*MoO_3 is strongly n-type,*

-After deposition in ultra high vacuum of MoO₃, IE = 9.7 eV, χ = 6.7 eV and WF = 6.9 eV.

-When deposited by classical thermal sublimation the films are systematically oxygen deficient, MoOx, they are semiconductor.

-Strongly reduced films, tends toward metallic conductivity.

-The WF value depends strongly on the composition and on the contamination of the films, it decreases with the reduction of the MoO₃ layers.

However, whatever is this value, the MoO_3 layer being strongly n-type, the IE and χ values are systematically high and the hole collection cannot be effective through its valence band, but through the conduction band. Moreover the presence of band gap states due to oxygen deficiency, not only decreases the resistivity of the film but also provides a second path for carrier exchange between the electrode and the organic material. So it cannot be a selective layer for electrons, which justifies that, in some specific conditions it can also be efficient as CBL. About its success as ABL, if it is due to the high value of IE, χ and WF, the decrease of these values due to reduction of the films (deposition conditions, contamination) is not harmful to the effect of the MoO_3 layer, because this decrease is associated with an increase of the density of states in the band gap what open a second pathway for the carriers and so compensates for the losses owed in change of the values of IE, χ and WF.

About its effect as CBL, due to the high values of IE, χ and WF it can be efficient only if very specific conditions are filled. These conditions, presence of high dipole at the interfaces, high concentration of gap states, to obtain electron paths, seem to be filled when the films are deposited by the hot wire technique. When evaporated, our study shows that these conditions are not filled, while they seem to be in the case of Jin et al [53]. It is known that IE, χ and WF and the density of gap states depends strongly on the deposition conditions and contamination of the MoO_3 films. Therefore, probably, the experimental and storing conditions are different. Our OPV cells were studied immediately after realisations without any ageing effect, which must correspond to high IE, χ and WF values and the formation of a high barrier at the interface fullerene/aluminium, while in the case of Jin et al, they proceed to long-term lifetime study and probably the values of IE, χ and WF are sensibly smaller which can justify a possible positive effect of MoO_3 CBL.

6. CONCLUSIONS

A review of the literature on MoO_3 buffer layer in organic optoelectronic devices confirms that, to day, MoO_3 appears as the best anode buffer layer. Indeed, in the case of OPV cells, whatever the deposition conditions and surface contamination are, it permits optimizing their efficiency, at least when the HOMO of the donor is less than 6 eV, which corresponds to the majority of the organic donors. This MoO_3 efficiency as ABL is due to the very high values of IE, χ and WF, and to the compensating effect of the gap states creation when the oxygen concentration in the films decreases or when the films are contaminated. Actually, this increase in the band gap states density in the forbidden bandgap allows opening a second pathway for the carriers and so compensates for the losses owed in change of the values of IE, χ and WF. About the use of MoO_3 as cathode buffer layer, it appears more unpredictable due to the fact that it must exhibits very specific properties to be efficient.

7. REFERENCES

[1] J. Meyer, S. Hamwi, M. Kröger, W. Kowalsky, T. Riedl, A. Kahn, *Transition metal oxides for organic electronic: Energetics, device physics and applications*, Adv. Mater. 24 (2012) 5408-5427.

[2] S. K. Deb, J. A. Chopoorian, *Optical properties and color-center formation in thin films of molybdenum trioxide*, J. Appl. Phys. 37 (1966) 4818-4825.

[3] N. Miyata, S. Akiyoshi, *Preparation and electrochromic properties of rf-sputtered molybdenum oxide films*, J. Appl. Phys. 58 (1985) 1651-1655.

[4] P.F. Carcia, E. M. McCarron, *Synthesis and properties pf thin film polymorths of molybdenum trioxide*, Thins Solid Films, 155 (1987) 53-63.

[5] A. F. Jankowski, L. R. Schrawyer, *Reactive sputtering of Molybdenum*, Thin Solid Films 193/194 (1990) 61-71.

[6] A. Abdllaoui, L. Martin, A. *Donnadieu, Structure and optical properties of MoO₃ thin films prepared by chemical vapor deposition,* Phys. Stat. Sol. (a) 109 (1988) 455- 462.

[7] A. Abdllaoui, G. Lévêque, A. Donnadieu, A. Bath, B. Bouchikhi, *Iteratively derived optical constants of MoO₃ polycrystalline thin films prepared by CVD*, Thin Solid Films 304 (1997) 39-44.

[8] M. Regragui, A. Donnadieu, *Caractérisation électrique et optique de couches minces de WO₃ et MoO₃ préparées par decomposition en phase vapeur (CVD)* J. Phys. III 2 (1992) 383-394.

[9] W. M. R. Divigalpitiya, R. F. Frindt, S. R. Morrison, *Oriented films of molybdenum trioxide*, Thins Sold Films 188 (1990) 173-179.

[10] Z. K. Alaoui, J. C. Bernède, J. Pouzet, *Textured binary compound thin films obtained by substitution of*

the chalcogen of pre-textured chalcogenide film, Vacuum 46 (1995) 373-378.

[11] P. A. Spevack, N. S. McIntyre, *Thermal reduction of MoO₃*, Journ. Phys. Chem. 96 (1992) 9029-9035.

[12] T. C. *Arnoldussen, Electrochromism and photochromism in MoO₃ films*, J. Electrochem. Soc: Solid State Science and Technology 123 (1976) 527-531.

[13] O. Zelaya-Angel, C. Menezes, F. Sanchez_Sinencio, *Electron diffusion and electrochromism in MoO₃ amorphous films*, J. Appl. Phys. 51 (1980) 6022-6026.

[14] R. R. Søndergaard, M. Hösel, F. C. Krebs, Roll-to-Roll *Fabrication of Large Area Functional Organic Materials*, J. Polymer Science B: Polymer Physics, 51 (2013) 16-34.

[15] M.-S. Kim, J.-S. Kim, J.C. Cho, M. Shtein, L.J.Guo, J. Kim, *Flexible conjugated polymer photovoltaic cells with controlled heterojunctions fabricated using nanoimprint lithography*, Appl. Phys. Lett. 90 (2007) 123113.

[16] R. Fitzner, C. Elschner, M. Weil, C. Uhrich, C. Körner, M. Riede, K. Leo, M. Pfeiffer, E. Reinold, E. Mena-Osteritz, P. Bäuerle, *Interrelation between Crystal Packing and Small-Molecule Organic Solar Cell Performance*, Adv. Mater. 24 (2012) 675-680.

[17] B.P. Rand, J. Li, J. Xue, R.J. Holmes, M.E. Thompson, S.R. Forrest, *Organic Double-Heterostructure Photovoltaic Cells Employing Thick Tris(acetylacetonat)ruthenium(III) Exciton-Blocking Layers*, Adv. Mater. 17 (2005) 2714-2718.

[18] J.C. Bernède, Y. Berredjem, L. Cattin, M. Morsli, *Improvement of organic solar cells performances using a zinc oxide anode coated by an ultra thin metallic layer*, Appl. Phys. Lett. 92 (2008) 083304.

[19] J.C. Bernède, L. Cattin, M. Morsli, Y. Berredjem, *Ultra thin metal layer passivation of the transparent conductive anode in organic solar cells*, Sol. Energy Mater. Sol. Cells, 92 (2008) 1508-1515.

[20] J. C. Bernède, D.-T. Nguyen, L. Cattin, M. Morsli, S.R.B. Kanth, and S. Patil, *About the transparent electrode of the organic photovoltaic cells*, Eur. Phys. J. Appl. Phys. 56 (2011) 34102.

[21] J. C. Bernède, L. Cattin, S. Ouro Djobo, M. Morsli, S. R. B. Kanth, S. Patil, P. Leriche, J. Roncali, A. Godoy, F. R. Diaz, and M. A. del Valle, *Influence of the highest occupied molecular orbital energy level of the donor material on the effectiveness of the anode buffer layer in organic solar cells*, Phys. Status Solidi A 208 (2011) 1989–1994.

[22] X.-Y. Jiang, Z.-L. Zhang, J. Cao, M.A. Khan, K.-ul-Haq, W.-Q. Zhu, *White OLED with high stability and low driving voltage based on a novel buffer layer MoOx*, J. Phys. D: Appl. Phys. 40 (2007) 5553-5557.

[23] H. You, Y. Dai, Z. Zhang, D. Ma, *Improved performances of organic light-emitting diodes with metal oxide as anode buffer*, J. Appl. Phys. 101, (2007) 26105.

[24] I. Yoo, M. Lee, C. Lee, D.-W. Kim, I. S. Moon, D.-H. Hwang, *The effect of a buffer layer on the photovoltaic properties of solar cells with P3OT:fullerene composites*, Synthetic Metals 153 (2005) 97-100.

[25] M. Y. Chan, C. S. Lee, S. L. Lai, M. K. Fung, F. L. Wong, H. Y. Sun, K. M. Lau, S. T. Lee, *Efficient organic photovoltaic devices using a combination of exciton blocking layer and anodic buffer layer*, J. Appl. Phys. 100 (2006) 094506.

[26] L. Cattin, F. Dahou, Y. Lare, M. Morsli, R. Tricot, K. Jondo, A. Khelil, K. Napo, J.C. Bernède, *MoO₃ surface passivation of the transparent anode in organic solar cells using ultra-thin films*, J. App. Phys. 105 (2009) 034507.

[27] M. Gacitua, Y. Boutaleb, L. Cattin, S. Yapi Abe, Y. Lare, G. Soto, G. Louarn, M Morsli, R. Rehamnia, M. A. del Valle, A. Drici, and J. C. Bernède, *Electrochemical preparation of MoO3 buffer layer deposited onto the anode in organic solar cells*, Phys. Status Solidi A 207 (2010) 1905–1911.

[28] J. Hwang, A. Wan, A. Kahn, *Energitics of metal-organic interfaces: New experiments and assessment of the field*, Mater. Science and Engin. R 64 (2009) 1-31.

[29] X. Crispin, *Interface dipole at organic/metal interfaces and organic solar cells*, Solar Energy Materials & Solar Cells 83 (2004) 147-168.

[30] Th. Kugler, W. R. Salaneck, H. Rast, A. B. Holmes. *Polymer band alignment at the interface with indium tin oxide: consequences for light emitting devices*, Chem. Phys. Lett. 310 (1999) 391-592.

[31] H. Vasquez, R. Oszwaldowski, P. Pou, J. Ortega, R. Perz, F. Flores, A. Khan, *Dipole formation at metal/PTCDA interfaces: Role of the charge neutrality level*, Euro Phys Lett. 65 (2004) 802-808.

[32] M. Kröger, S. Hamwi, J. Meyer, T. Riedl, W. Kowalsky, A. Khan, *Role of the deep-lying electronic states of MoO3 in the enhancement of hole-injection in orgtanic thin films*, Appl. Phys. Lett. 95 (2009) 123301.

[33] T. S. Sian, G. B. Reddy, *Optical, structuraland photoelectron spectroscopic studies on amorphous and crystalline molybdenum oxide thin films*, Sol. Energy Mater. and Sol. Cells, 82 (2004) 375-386.

[34] M. T. Greiner, M. H. Helander, Z. B. Wang, W. M. Tang, J. Qiu, Z. H. Lu, *A metallic molybdenum suboxide buffer layer for organic electronic devices*, Appl. Phys. Lett. 96 (2010) 213302.

[35] I. Irfan, H. Ding, Y. Gao, C. Small, D. Y. Kim, J. Subbiah, F. So, *Energy level evolution of air and oxygen exposed molybdenum trioxide films*, Appl. Phys. Lett. 96 (2010) 243307.

[36] J. Mayer, A. Shu, M. Kröger, A. Khan, *Effect of contamination on the electronic structure and hole-injection properties of MoO₃/organic semiconductor interfaces*, Appl. Phys. Lett. 96 (2010) 133308.

[37] M. C. Gwinner, R. Di Pietro, Y. Vaynzof, K. J. Greenberg, P. K. H. Ho, R. H. Friend, H. Sirringhaus, *Doping of organic semiconductors using molybdenum trioxide: a quantitative time-dependent electrical and spectroscopic study*, Adv. Funct. Mater. 21 (2011) 1432-1441.

[38] J. Q. Zhong, H. Y. Mao, R. Wang, J. D. Lin, Y. B. Zhao, J. L. Zhang, D. G. Ma, W. Chen, *Ionization potential dependent air exposure effect on the MoO3/organic interface energy level alignment*, Organic Electronics 13 (2012) 2793-2800.

[39] X. Tong, B. E. Lassiter, S. R. Forrest, *Inverted organic photovoltaic cells with high open-circuit voltage*, Organic Electronics 11 (2010) 705-709.

[40] M. G. Varnamkhasti, H. R. Fallah, M. Mostajaboddavati, R. Ghasemi, A. Hassanzadeh, *Comparison of metal oxides as anode buffer layer for small molecule organic photovoltaic cells*, Solar Energy Materials & Solar Cells 98 (2012) 379-384.

[41] J-Y. Sun, W-H. Tseng, S. Lan, S-H. Lin, P-C. Yang, C-I Wu, C-F. Lin, *Performance enhancement in inverted polymer photovoltaics with solution-processed MoOx and air-plasma treatment for anode modification*, Solar Energy Materials & Solar Cells 109 (2013) 178-184.

[42] J. C. Bernède, S. Houari, D. Nguyen, P. Y. Jouan, A. Khelil, A. Mokrani, L. Cattin, P. Predeep, *XPS study of the band alignment at ITO/oxide (n-type MoO3 or p-type NiO) interface*, Phys. Status Solidi A 209 (2012) 1291–1297.

[43] A. Buckley, D. Pickup, C. Yates, Y. Zhao, D. Lidzey, *Hole injection in tri-arylamine containing polyfluorene co-polymer devices with molybdenum oxide contacts*, J. Appl. Phys. 109 (2011) 084509.

[44] S. W. Cho, L. F. J. Piper, A. DeMasi, A. R. H. Preston, K. E. Smith, K. V. Chauhan, R. A. Hatton, T. S. Jones, Soft *X-ray spectroscopy of C69/Copper phthalocyanine/MoO3 interfaces: Role of reduced MoO3 on energetic band alignment and improved performance*, J. Phys. Chem. C 114 (2010) 18252-18257.

[45] P. Jeon, K. Han, H. Lee, H. S. Kim, K. Jeong, K. Cho, S. W. Cho, Y. Yi, *The origin of hole injection improvements with MoO2/Al bilayer electrodes in pentacene thin-film transistors*, Synthetic Metals, 158 (2009) 2502-2505.

[46] Y. Zhao, J. Chen, W. Chen, D. Ma, Poly(3, 4-ethylenedioxythiophene):poly(styrenesulfonate)/MoO3 *composite layer for efficient and stable hole injection in organic semiconductors*, J. Appl. Phys. 111 (2012) 043716.

[47] C-T. Lin, C-H. Yeh, M-H. Chen, S-H. Hsu, C-I Wu, T-W. Pi, *Influences of evaporation temperature on electronic structures and electrical properties of molybdenum oxide in organic light emitting devices*, Appl. Phys. Lett. 107 (2010) 053703.

[48] S. Y. Chiam, B. Dasgupta, D. Soler, M. Y. Leung, H. Liu, Z. E. Ooi, L. M. Wong, C. Y. Jiang, K. L. Chang, J. Zhang, *Investigating the stability of defects in MoO3 and its role in organic solar cells*, Sol. Energy Mater. and Sol. Cells, 99 (2012) 197-203.

[49] P-S. Wang, I-W. Wu, W-H. Tseng, M-H. Chen, C-I Wu, *Enhancement of current in organic light emitting diodes with sputter treated molybdenum oxides as hole injection layers*, Appl. Phys. Lett. 98 (2011) 173302.

[50] J-Y. Sun, W-H. Tseng, S. Lan, S-H. Lin, P-C. Yang, C-I Wu, C-F. Lin, *Performance enhancement, in inverted polymer photovoltaics with solution-processed MoOx and air-plasma treatment for anode modification*, Sol. Energy Mater. and Sol. Cells, 109 (2013) 178-184.

[51] M. Vasilopoulou, L. C. Palilis, D. G. Georgiadou, P. Argitis, S. Kennou, L. Sygeliou, I. Kostis, G. Papadimitropoulos, N. Konofaos, A. A. Liadis, D. Davazoglou, *Reduced molybdenum oxide as an efficient electron injection layer in polymer light-emitting diodes*, Appl. Phys. Latt. 98 (2011) 123301.

[52] M. Vasilopoulou, L. C. Palilis, D. G. Georgiadou, , S. Kennou, I. Kostis, D. Davazoglou, P. Argitis, *Barrierless hole injection through sub-bandgap occupied states in organic light emitting diodes using substoichiometric MoOx anode interfacial layer*. Appl. Phys. Latt. 100 (2012) 013311.

[53] F. Jin, B. Chu, W. Li, Z. Su, B. Zhao, X. Yan, F. Zhang, D. Fan, T. Zhang, Y. Gao, C. S. Lee, J. Wang, *Improvement in power conversion efficiency and long-term lifetime of organic photovoltaic cells by using bathophenanthroline/ molybdenum oxide as compound cathode buffer layer*, Sol. Energy Mater. and Sol. Cells, 117 (2013) 189-193.

[54] B. Kouskoussa, M. Morsli, K. Benchouk, G. Louarn, L. Cattin, A. Khelil, J. C. Bernède, *On the improvement of the anode/organic material interface in organic solar cells by the presence of an ultra-thin gold layer*, Phys. Status Solidi A 206 (2009) 311–315.

[55] Y. Lare, B.Kouskoussa, K.Benchouk, S.OuroDjobo, L.Cattin, M.Morsli, F.R.Diaz, M.Gacitua, T. Abachi, M.A.delValle, F.Armijo, G. A.East, J.C.Bernède, *Influence of the exciton blocking layer on the stability of layered organic solar cells*, J. Phys. Chem. Solids 72 (2011) 97–103.